Bull. Mater. Sci., Vol. 39, No. 7, December 2016, pp. 1685–1690. © Indian Academy of Sciences.
DOI 10.1007/s12034-016-1306-8

Effect of stabilizer on the morphology of Au@TiO_2 spheres: a combined experimental and theoretical study

JIAN QI[1,*], XUECHAO GAO[2] and QUAN JIN[1]

[1]National Key Laboratory of Biochemical Engineering, Institute of Process Engineering, Chinese Academy of Sciences, Beijing 100190, People's Republic of China

[2]Ningbo Institute of Materials Technology and Engineering, Chinese Academy of Sciences, Ningbo, Zhejiang 315201, People's Republic of China

MS received 28 January 2016; accepted 15 April 2016

Abstract. **In this study, two different particle sizes of Au nanoparticles (NPs) were synthesized using two different stabilizers, and then two different morphologies Au@TiO_2 hollow spheres were obtained when the corresponding Au NPs solutions were added to the TiF_4 ethanol–water solution under hydrothermal condition. The computational simulation is employed to provide the fundamental support to explain why different stabilizers yield different sizes of Au NPs, and the main cause for the experimental observation is contributed by the different interactive forces between Au and stabilizer molecules. The experimental strategy adopted different stabilizer in this work is expected to be generally applicable for the synthesis of many other types of micro-nanostructured materials.**

Keywords. **Au nanoparticle; stabilizer; interaction force; Au@TiO_2; hollow spheres.**

1. Introduction

Micro-nanostructured semiconductor materials with tunable morphology and size by chemical synthetic methods are of great interest for extensive applications, such as energy conversion and storage, sensors, catalysis, drug delivery, and so on [1]. Among the semiconductor material families, titania (TiO_2) with wide bandgap as an important member has been paid extensive attention and application due to its low cost and high availability, non-toxicity, harmless, chemical stability and environmentally friendly [2]. However, for some photocatalytic reactions, the reaction rate of TiO_2 is lower and significantly limited in practical application. Hence, it is necessary to search the novel method for improving the reaction rate of TiO_2. Noble metal Au nanoparticles (Au NPs) as an excellent electron capture agents can form schottky barrier with TiO_2 that can capture photo-generated electrons, which remarkably improves the catalytic activity of TiO_2 [3,4]. In addition, Au NPs on the TiO_2 surface can further increase the light absorption due to strong surface plasmon resonances [5]. Therefore, Au NPs–TiO_2 composite materials will undoubtedly expand the spectral response range of TiO_2 material. On the other hand, the morphology and size of Au NPs will have an effect on the intensity of surface plasmon resonance, thus it is necessary to control the morphology and size of Au NPs to optimize its performance. In general, the size of Au NPs can be controlled by adjusting the amount of gold source [6,7], but the influence from stabilizers are little actually concerned, and there is always the possibility that the kinds of stabilizer in the synthesis system would significantly affect the size-dependent property of Au NPs. In the present study, we have adopted trisodium citrate and 3-mercaptopropionic acid as the stabilizers to prepare different Au NPs, and then added titanium source (TiF_4) to synthesize Au–TiO_2 composite by hydrothermal method. In addition, the computational simulation is adopted and contributed to understand why different stabilizer has different influences on the size of Au NPs, and further affects the morphology of the Au–TiO_2 composite.

2. Experimental

2.1 *Synthesis of Au NPs with trisodium citrate as stabilizer*

An aqueous solution of $HAuCl_4 \cdot 3H_2O$ (10 mM, 2.5 ml) was added to deionized water (95 ml) and stirred for 2 min. A trisodium citrate solution (10 mM, 2.5 ml) was then added, and the resulting mixture was kept for 10 min under stirring. Finally, $NaBH_4$ (100 mM, 1.5 ml) was added and the mixture was continuously stirred for 10 h.

2.2 *Synthesis of Au NPs with 3-mercaptopropionic acid as stabilizer*

An aqueous solution of $HAuCl_4 \cdot 3H_2O$ (10 mM, 2.5 ml) was added to deionized water (95 ml) and stirred for 2 min. 3-Mercaptopropionic acid (10 mM, 2.5 ml) was then added, and the obtained mixture was kept for 10 min under stirring. Finally, $NaBH_4$ (100 mM, 5 ml) was added and the mixture was further stirred for 10 h.

J Q and X G contributed equally to this study.

*Author for correspondence (jqi@ipe.ac.cn)

2.3 *Synthesis of Au@TiO_2 hollow submicrospheres with trisodium citrate as stabilizer*

The prepared Au NPs solution (3 ml, trisodium citrate as stabilizer) was sequentially mixed with water (21 ml) and ethanol (21 ml), and the reaction mixture was stirred for 10 min at room temperature. Subsequently, TiF_4 (40 mM, 3 ml) was added, and the obtained mixture was kept for 30 min under stirring. Finally, the mixture was transferred to teflon-lined stainless steel autoclaves and heated to 180°C for 8 h. The obtained solid product was centrifuged, then washed three times with distilled water, and dried in air at room temperature.

2.4 *Synthesis of Au@TiO_2 hollow submicrospheres with 3-mercaptopropionic acid as stabilizer*

The prepared Au NPs solution (3 ml, 3-mercaptopropionic acid as stabilizer) was sequentially mixed with water (21 ml) and ethanol (21 ml), and the reaction mixture was stirred for 10 min at room temperature. Subsequently, TiF_4 (40 mM, 3 ml) was added, and the obtained mixture was kept for 30 min under stirring. Finally, the mixture was transferred to teflon-lined stainless steel autoclaves and heated to 180°C for 8 h. The resultant solid product was centrifuged, washed three times with distilled water, and dried in air at room temperature.

2.5 *Characterization*

Powder X-ray diffraction (XRD) patterns were recorded on a Panaltical X'Pert-pro MPD X-ray power diffractometer, using CuKα radiation ($\lambda = 1.54056$ Å). Scanning electron microscopy (SEM) procedure was performed on a Hitachi S-4800 electron microscope and transmission electron microscopy (TEM) was performed on a FEI Tecnai G^2 F20 electron microscope operated at 200 kV with the software package for automated electron tomography. UV–vis spectra were recorded on a Hitachi Model U-3010 spectrophotometer.

3. Results and discussion

As shown in figure 1A and B, when trisodium citrate and 3-mercaptopropionic acid are used as stabilizers, the sizes of Au NPs are 3.03 ± 0.56 nm (defined as Au@TSC, based on 65 counts) and 2.31 ± 0.38 nm (defined as Au@3-MPA, based on 65 counts), respectively. It is evident that the size of Au@3-MPA is smaller than that of Au@TSC. Figure 1c shows the UV–visible absorption spectra and photographs of the two kinds of Au NPs solutions. For Au@TSC NPs, characteristic absorption peak occurs at 520 nm, while it is inconspicuous for Au@3-MPA due to its smaller size.

In order to explain why the size of Au@3-MPA is smaller than that of Au@TSC, the interactive forces between Au and trisodium citrate, and between Au and 3-mercaptopropionic acid are calculated using a density functional theory method in Gaussian 09 software package [8]. In this method, all the structural optimizations were conducted using the B3LYP hybrid functional, in which the exchange functional is the combination of the Becke's three-parameter formulation and the gradient-corrected correlation, LYP, of Lee, Yang and Parr [9,10]. The basis sets are crucial to accurately evaluate the intramolecular energy, thus mixed basis sets were employed for different atoms in the molecules, i.e., a 6-311G (2d, p) polarized basis set is used for the trisodium citrate (atoms: C, H, O and Na) and 3-mercaptopropionic acid (atoms: C, H, O and S), in addition, a LanL2DZ basis set is employed for Au atoms in order to include the effective core potentials in heavy metal elements. Furthermore, the counterpoise method is further used to consider the basis set superposition error effect in the later intramolecular interaction. The interaction energy (E_{ab}) between the two fragments is generally defined by the following formula [11,12].

$$E_{ab} = E_{\text{Au/fragment}} - (E_{\text{Au}} + E_{\text{fragment}}), \tag{1}$$

in which E_{Au} and E_{fragment} are the single point energy (SP) for Au atom and fragment (trisodium citrate or 3-mercaptopropionic acid), and $E_{\text{Au/fragment}}$ is the total energy for the supramolecule of Au-fragments.

It is evident that the intramolecular interaction is significantly dependent on the interacting site in the fragment molecules. To take this effect into account, figure 2 provides several possible interacting sites in the molecules, and the corresponding obtained intramolecular energy and the interacting distance are listed in table 1.

As shown in table 1, for the same functional group in trisodium citrate molecule, the energy intensity is inversely proportional to the distance between the Au atom and functional group, with closer distance yielding higher binding energy. The strongest interacting energy is yielded by position II, having a value of 49.32 kJ mol^{-1}. In addition, for the different functional group in 3-mercaptopropionic acid, although the interacting distance is identical, the intramolecular energy dramatically differs with each other, indicating that the thiol group (−SH, 31.75 kJ mol^{-1}) in position I produces higher interacting energy than the carboxyl group does (−COOH, 9.80 kJ mol^{-1}), suggesting the binding energy is very sensitive to the interacting groups. Furthermore, based on the above results, it is safe to conclude that the interaction effect in trisodium citrate with Au NPs in the solution is mainly produced by carboxyl group in position II, and the thiol group dominates the interaction effect between 3-mercaptopropionic acid and Au NPs in the solution. In addition, to compare the intramolecular energy intensity between different molecules, the corresponding molecular size effect of the fragments must be taken into account due to the limited accessible volume around the Au NPs surface, thus the interaction energy density, $\rho(E_{\text{ab}})$, is proposed as below

$$\rho(E_{\text{ab}}) = \frac{E_{\text{ab}}}{V_{\text{fragment}}}, \tag{2}$$

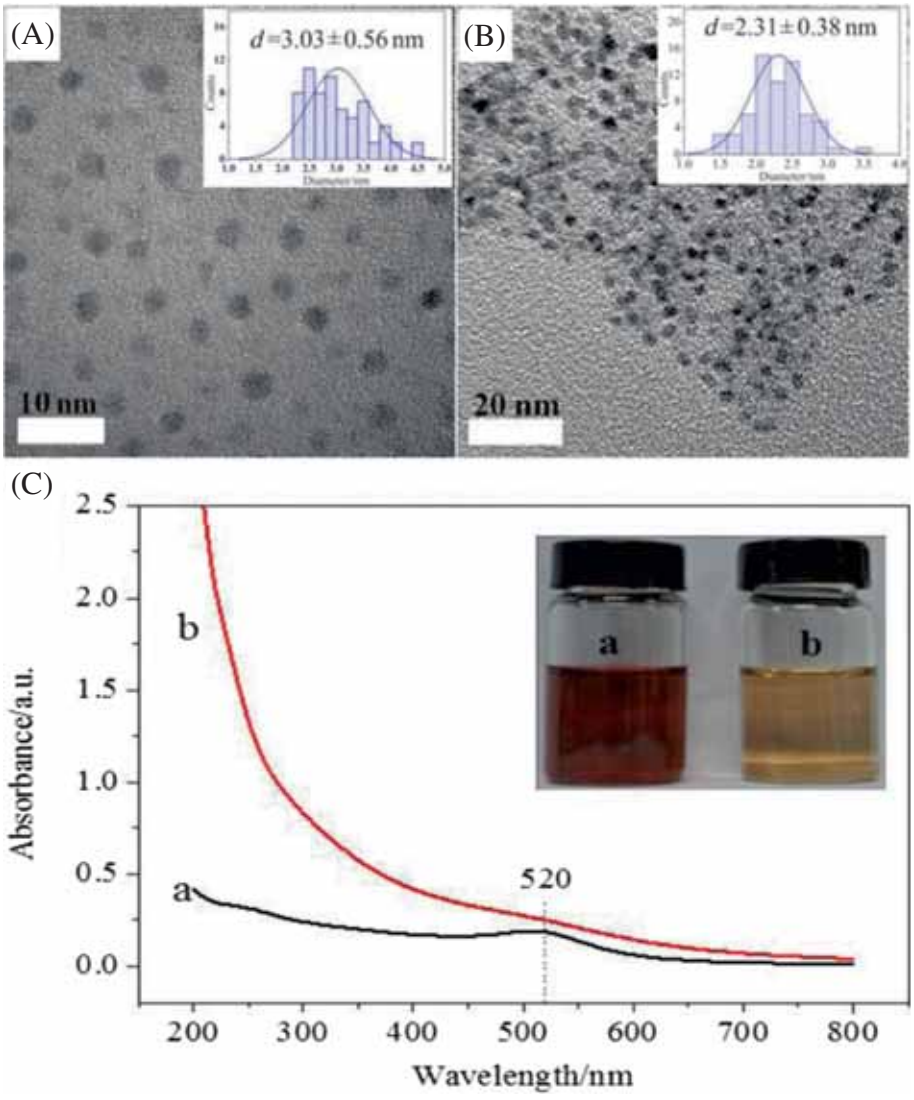

Figure 1. TEM images of Au NPs with different stabilizers: (**A**) trisodium citrate, (**B**) 3-mercaptopropionic acid and (**C**) UV–visible spectra and photographs of the obtained corresponding Au NPs solutions.

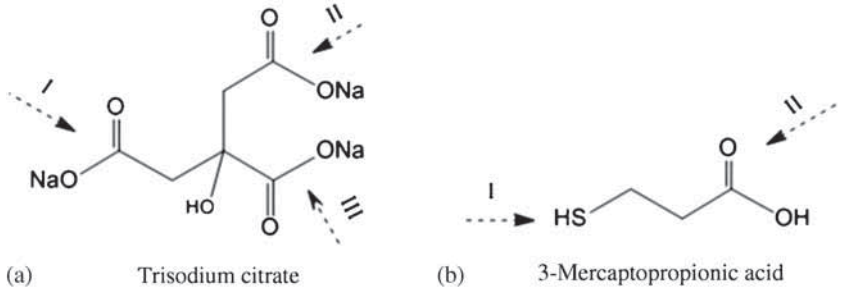

Figure 2. The possible approaching direction of Au atoms to interact with the functional groups in the stabilizers: (**a**) trisodium citrate and (**b**) 3-mercaptopropionic acid.

in which $V_{fragment}$ is the Van der Waals volume of the two stabilizing molecules. The corresponding values were also evaluated in Gaussian 09 via the same method and basis set. The obtained volumes of trisodium citrate and 3-mercaptopropionic acid molecules are 135.321 and 77.286 cm^3 mol^{-1}, respectively, thus the corresponding strongest interaction

Table 1. Interacting sites in the stabilizers and the corresponding intramolecular interaction energy with Au NPs.

Interacting site	E_{ab} (kJ mol^{-1})	d (Au–M) M = O, S (Å)
Trisodium citrate–Au(I)	22.60	2.481
Trisodium citrate–Au(II)	49.32	2.381
Trisodium citrate–Au(III)	33.56	2.423
3-Mercaptopropionic acid–Au(I)	31.75	2.667
3-Mercaptopropionic acid–Au(II)	9.80	2.644

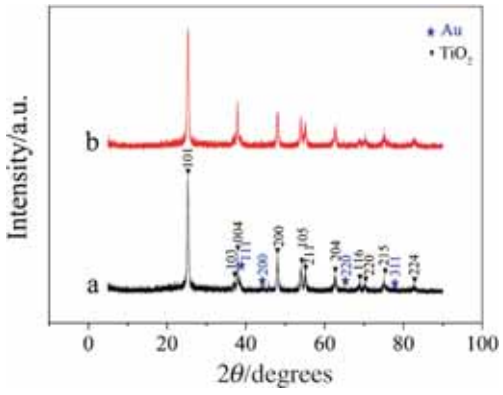

Figure 3. XRD patterns of Au@TiO_2 hollow submicrospheres with different stabilizers: (**a**) trisodium citrate and (**b**) 3-mercaptopropionic acid.

energy intensity, $\rho(E_{ab})$, in the two fragments is 0.365 and 0.411 kJ cm^{-3}, respectively. Therefore, it is safe to derive that the intermolecular interaction between 3-mercaptopropionic acid and Au NPs is stronger due to more molecules filled in the effective surrounding volume, which prevents the Au atoms from further aggregating and crystallizing in the solution during the reaction, thus smaller Au NPs are observed in figure 1.

The crystal structures of the two kinds of Au@TiO_2 hollow submicrospheres are further discerned by XRD patterns (figure 3). Both the samples show 11 distinct peaks, indexable as (101), (103), (004), (200), (105), (211), (204), (116), (220), (215) and (224) lattice planes (black triangle), which are the characteristic of the anatase crystal phase (JCPDS PDF#: 00-021-1272) [13], and (111), (200), (220) and (311) lattice planes are attributed to face-centered cubic Au (blue five-pointed star). It is also observed that the peak intensity of Au phase with 3-mercaptopropionic acid as stabilizer becomes smaller compared with trisodium citrate as stabilizer. This is reasonable because the sizes of Au@3-MPA NPs are smaller than that of Au@TSC NPs. Meanwhile, the interaction force is stronger between Au and 3-mercaptopropionic acid than that of Au and trisodium citrate, which leads to smaller NPs during hydrothermal synthesis to prepare Au@TiO_2 composite.

It is generally accepted that the hydrothermal synthesis is a green, simple and cheap method and widely used for the synthesis of micro-/nano materials. In this study, Au@TiO_2 nanostructure composite is synthesized by heating the mixture of Au NPs, Ti precursors, ethanol and water at 180°C for 8 h under the hydrothermal condition. The morphology and structure of as-prepared Au@TiO_2 nanostructure composite are explored by SEM and TEM. Several important features can be discerned: (1) figure 4 displays typical SEM image and TEM of Au@TiO_2 nanostructure composite. When trisodium citrate is used as the stabilizer, Au@TiO_2 hollow spheres have better monodispersity. The spheres consist of Au nano-particle of approximately 30–50 nm in diameter, which is individually encased in TiO_2 hollow sphere having a diameter of 300–600 nm and a wall thickness of 60–90 nm (figure 4a–c). However, when 3-mercaptopropionic acid is selected as the stabilizer, Au@TiO_2 hollow spheres have poor monodispersity compared with trisodium citrate as stabilizer, and the hollow spheres are linked to each other. In addition, the observed spheres consist of Au nano-particle of approximately 5–10 nm in diameter, which is individually encased in TiO_2 hollow sphere having a diameter of 300–500 nm and a wall thickness of 60–80 nm. On the other hand, it is evident that the size of Au NPs changes in Au@TiO_2 nanostructure composite are considerably different between two kinds of Au@TiO_2 hollow spheres. For trisodium citrate as the stabilizer, the size of Au NPs changes from 3 to 30–50 nm during hydrothermal condition, while the size of Au NPs changes from 2 to 5–10 nm for 3-mercaptopropionic acid as stabilizer. The main cause is that the interaction force between Au NP and 3-mercaptopropionic molecule is stronger than that of interaction force between Au NP and trisodium citrate. During hydrothermal reaction process, the Au NPs stabilized by trisodium citrate are easier to aggregate and grow into larger particles due to weaker interaction force between Au NP and trisodium citrate. However, the Au NPs stabilized by 3-mercaptopropionic molecule are harder to grow due to the 'shield' effect provided by the stronger interaction force between Au NP and 3-mercaptopropionic molecule, thus smaller Au particles occurred. The experimental phenomenon indicates that, in addition to the crystallization reaction temperature, the size of the Au NPs is strongly dependent on the stabilizer. On the whole, with the hydrothermal crystallization process proceeding, when the amorphous solid TiO_2 nanocrystallites gradually dissolve and form hollow structure, the embedded Au NPs located in the amorphous TiO_2 matrix begin to migrate and aggregate into big Au NPs in the cavity resulting from without the protection of TiO_2 particles. How did the hollow structure form? We consider that during hydrothermal crystallization process, the amorphous solid Au@TiO_2 spheres composed of numerous smaller nanocrystallites were formed first. Compared to the nanocrystallites in the outer surfaces, the size and crystallinity of the nanocrystallites located in the inner are smaller and lower, which make them have higher curvatures and high surface energies and easy to be dissolved into the surrounding medium, and then re-deposited on the surface of outer larger NPs, which makes the outer particles grow gradually [14]. When the crystallization time is

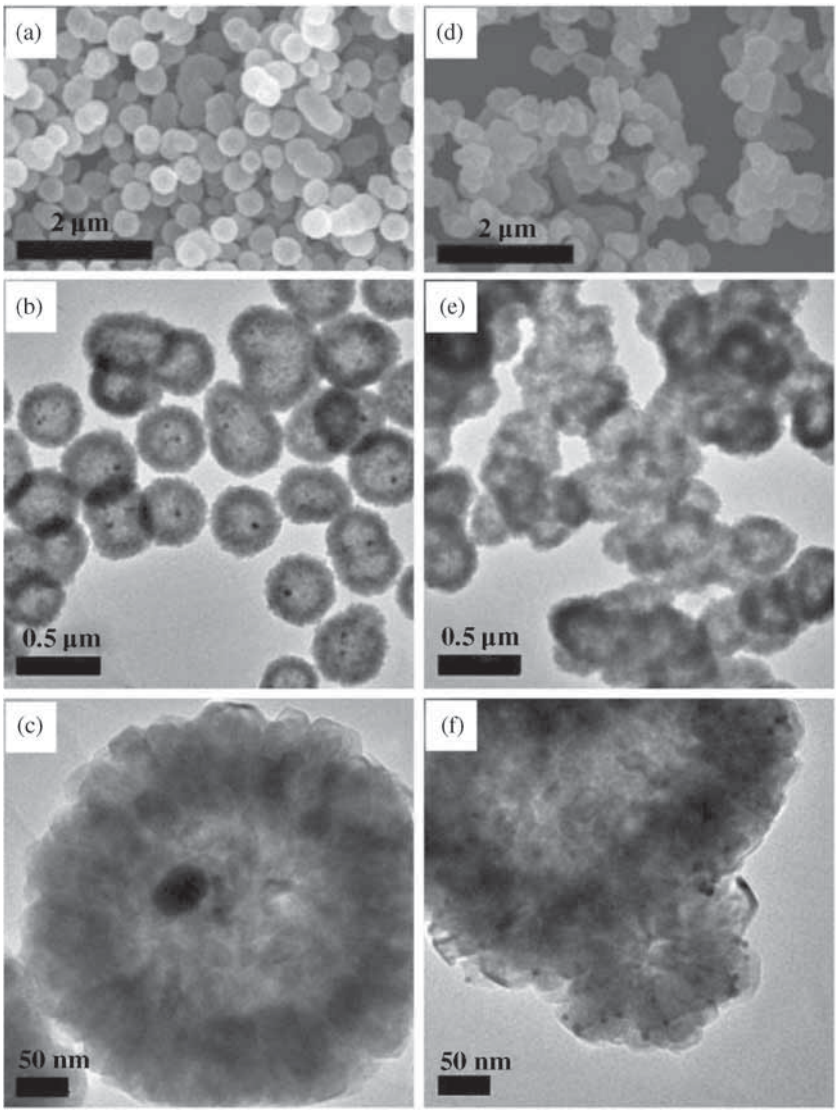

Figure 4. SEM and TEM of Au@TiO_2 hollow submicrospheres with different stabilizers: (**a**–**c**) trisodium citrate and (**d**–**f**) 3-mercaptopropionic acid.

longer, the edges of the Au@TiO_2 spheres transform into polycrystalline structure, meanwhile, the hollow structure of Au@TiO_2 spheres is formed. On the basis of the previous study, the Ostwald ripening process is believed to play an important role in the formation of hollow structure, and the formation mechanism is similar to other kinds of hollow structure micro-/nanomaterials [15].

In order to obtain the intermediate states of Au@TiO_2 spheres, the hydrothermal crystallization time was investigated. For trisodium citrate as the stabilizer, when the crystallization time is shortened to 1 h at 180°C, the intermediate product shows the spherical morphology with smaller size of 150–300 nm resulting from part of the TiF_4 reactant being not completely reacted (supplementary figure S1a). In addition, the surfaces of spheres are rough, which is mainly caused by the low crystallinity of spheres. As the crystallization time increases, the size and the surface of Au@TiO_2 spheres become larger and smooth because TiF_4 reactant is completely reacted and crystallinity of the product is improved (supplementary figure S1b–d). Similarly, for 3-mercaptopropionic acid as the stabilizer, with crystallization time increasing, the size and crystallinity of product become larger and higher (supplementary figure S1e–h). Thus it can be seen that the crystallization time is very important for the morphology of Au@TiO_2 spheres.

In order to expand the types of stabilizers, four kinds of different materials are chosen as stabilizers to synthesize Au NPs and Au–TiO_2 composite (see supplementary Information). The sizes of Au NPs with different stabilizers are 1.4–2.8 nm (supplementary figure S2a, PEI), 1.4–2.8 nm (supplementary figure S2b, PVA), 4.2–5.6 nm (supplementary figure S2c, PVP) and 4.2–14.7 nm (supplementary figure S2d, PEG), and the corresponding morphologies of Au–TiO_2 composite are strip shaped (supplementary figure S2e), solid core-shelled (supplementary figure S2f and g) and hollow core-shelled structure (supplementary figure S2h). Similarly,

after hydrothermal crystallization process, the sizes of Au NPs become larger, and the sizes are 6.8–20.6 nm (supplementary figure S2e, PEI), 3.4–10.3 nm (supplementary figure S2f, PVA), 6.8–13.6 nm (supplementary figure S2g, PVP) and 10.3–17.2 nm (supplementary figure S2h, PEG), respectively. Thus it can be seen that different stabilizers are very important for the morphology and size of Au–TiO_2 composite. Meanwhile, the synthetic strategy for the preparation of noble metal NPs with different stabilizer protection and noble metal/semiconductor composite materials provides some experimental basis.

In this study, the hollow structure as an ideal candidate has potential application in catalysis areas. For instance, the obtained hollow interior can act as an excellent light-harvesting space due to efficient light scattering and diffraction of different wavelengths, thus it is safe to conclude that the structural characteristics enhance the photo-conversion process, such as photo-catalysis and dye-sensitized solar cells.

4. Conclusions

In summary, two kinds of Au@TiO_2 hollow spheres with different morphologies and different size Au NPs are synthesized under hydrothermal condition. Different stabilizers yield different sizes of Au NPs, and the computational simulation is adopted and contributed to intensively understand why different stabilizer has different effect on the size of Au NPs, which further affects the morphology of the Au@TiO_2 composite. This is believed to be due to the different interaction forces between Au and stabilizers. The strategy adopted different stabilizer in this work is expected to be widely employed for synthesis of many types of micro-nanostructured materials.

Electronic Supplementary Material

Supplementary material pertaining to this article is available on the Bulletin of Materials Science website (www.ias.ac.in/matersci).

Acknowledgement

This study was supported financially by the National Natural Science Foundation of China (Grant nos 51572261 and 51502311), China Postdoctoral Science Foundation (Grant no. 2015M571909) and Natural Science Foundation of Ningbo (Grant no. 2015A610087).

References

[1] Qi J, Lai X Y, Wang J Y, Tang H J, Ren H, Yang Y, Jin Q, Zhang L J, Yu R B, Ma G H, Su Z G, Zhao H J and Wang D 2015 *Chem. Soc. Rev.* **44** 6749

[2] Ma Y, Wang X L, Jia Y S, Chen X B, Han H X and Li C 2014 *Chem. Rev.* **114** 9987

[3] Bannat I, Wessels K, Oekermann T, Rathousky J, Bahnemann D and Wark M 2009 *Chem. Mater.* **21** 1645

[4] Ding D W, Liu K, He S N, Gao C B and Yin Y D 2014 *Nano Lett.* **14** 6731

[5] Zheng Z K, Huang B B, Qin X Y, Zhang X Y, Dai Y and Whangbo M H 2011 *J. Mater. Chem.* **21** 9079

[6] Bian Z F, Tachikawa T, Zhang P, Fujitsuka M and Majima T 2014 *J. Am. Chem. Soc.* **136** 458

[7] Cheng L, Li X F and Dong J F 2015 *J. Mater. Chem. C* **3** 6334

[8] Frisch M J, Trucks G W, Schlegel H B *et al* 2009 Gaussian 09, Revision A. 02 (Wallingford, CT: Gaussian Inc.)

[9] Lee C, Yang W and Parr R G 1988 *Phys. Rev. B* **37** 785

[10] Hacarlioglu P, Lee D, Gibbs G V and Oyama S T 2008 *J. Membr. Sci.* **313** 277

[11] Lin Y, Zhang Q, Zhao C, Li H, Kong C, Shen C and Chen L 2015 *Chem. Comm.* **51** 697

[12] Murugan L, Lakshmipathi S and Bhatia S K 2014 *RSC Adv.* **4** 39576

[13] Zeng Q P, Li H, Duan H N, Guo Y P, Liu X F, Zhang Y Y and Liu H Z 2015 *RSC Adv.* **5** 13430

[14] Yang H G and Zeng H C 2004 *J. Phys. Chem. B* **108** 3492

[15] Yec C C and Zeng H C 2014 *J. Mater. Chem. A* **2** 4843